Proceedings of Global Power and Propulsion Society
ISSN-Nr: 2504-4400
GPPS Hong Kong 2023
October 17-19, 2023
www.gpps.global

GPPS-TC-2023-0260

Numerical Investigations on the Dynamical Behaviours of Flickering Buoyant Diffusion Flames in Externally Rotating Flows

Tao Yang
Department of Mechanical Engineering, The Hong Kong Polytechnic University
tao2021.yang@connect.polyu.hk
Hung Hom, Kowloon, Hong Kong

Yuan Ma
Department of Mechanical Engineering, The Hong Kong Polytechnic University
y.ma@polyu.edu.hk
Hung Hom, Kowloon, Hong Kong

Peng Zhang*
Department of Mechanical Engineering, City University of Hong Kong
penzhang@cityu.edu.hk
Kowloon Tong, Kowloon, Hong Kong

ABSTRACT

The flicker of a buoyant diffusion flame in rotating flows is computationally investigated, particularly focusing on the flame dynamical behaviors in a large rotating intension range. Diffusion flames are produced computationally and imposed in different rotating flows, which are generated by four wing walls. In the quiescent environment, the flicker frequency follows a scaling law of $f \sim \sqrt{g/D}$. With the rotating intension R enhancing, the buoyancy-induced oscillation becomes faster first and vanished finally. In the weakly rotating flow, the present computational and theoretical results show that the frequency increase correlates with R^2. When R is large, the local extinguishing causes the flame lift-off at the bottom. In the present study, six distinct flame modes including flickering, oscillating, steady, spiral, lifted, and vortex-bubble flames are found in the various rotating conditions. To further study the dynamical behaviors of different flame modes, phase portraits, as an invaluable tool, are illustrated.

INTRODUCTION

Diffusion flame is a crucial problem that concerns flame stability in industrial fields and fire safety in environmental fields. The buoyancy-driven “flickering” or “puffing” has been focused for several decades. Previous studies (Buckmaster & Peters, 1988; Chamberlin & Rose, 1948; Moreno-Boza et al., 2016; Xia & Zhang, 2018; Yang, Xia, & Zhang, 2019) found that flickering of flame is a well-known instability of buoyance-dominated diffusion flame, where buoyancy plays an important role to cause a self-sustained oscillating flame. In general, the flame is elongated vertically and contracted horizontally during one periodic oscillation. Accordingly, a flame “neck” or even pinch-off is formed at the flame top. From the perspective of vortex dynamics, Xia and Zhang (Xia & Zhang, 2018) established a unified vortex-dynamical theory to interpret the scaling frequency of single flickering buoyant diffusion flames; Yang et al. (Yang et al., 2019) computationally studied dual buoyant diffusion flames and proposed a characteristic Reynolds number for the transition between anti-phase and in-phase flickering modes; Yang et al. (Yang, Chi, & Zhang, 2022) interpreted vortex interactions in triple flickering buoyant diffusion flames for four distinct dynamical modes.

Flames can be stabilized by rotating flows, of which issues have been studied for a long time due to the relevant practices. Recent decades ago, many experiments (Cha & Sohrab, 1996; Gotoda, Asano, Chuah, & Kushida, 2009; Gotoda, Ueda, Shepherd, & Cheng, 2007; Sheu, Sohrab, & Sivashinsky, 1990) studied flame stabilization under different burner rotating conditions, in which the flame oscillating behaviors is induced by buoyancy. Gotoda and his coworkers (Gotoda et al., 2009; Gotoda et al., 2007), reported that the flame could retain the periodic flicker only when the rotational speeds are low. The flame would transition into low-dimensional deterministic chaos at very large rotating conditions, in which the flame oscillation is spiral. Lei et al. (Lei, Liu, & Satoh, 2015) observed that small-scale buoyant flames in rotating flows can exhibit higher pulsation frequencies than those in the quiescent environment. Subsequently, they also conducted many experimental studies on the dynamical behaviors of buoyant flames with swirling. In addition, Coenen et al. (Coenen, Kolb, Sánchez, & Williams, 2019) found that the strong external rotation could weaken the puffing instability of pool fires and form helical instability. However, there is limited literature on how a flickering flame behaves in a large range of rotating flows and underlying physical mechanisms.

This study aims to provide a vortex-dynamical analysis of the buoyance-induced flame flicker in an externally rotating flow. Detailed information on flow and temperature fields will be obtained by means of numerical simulation. In the weakly rotating flow, the flickering frequency correlation will be established and extended from the theory of Xia and Zhang (Xia & Zhang, 2018). In the large rotating intension range, different flame modes will be illustrated based on the phase portraits of velocity and temperature in flames. By analyzing the flame and vortex, we seek to understand the mechanisms of distinct flame modes.

METHODOLOGY

Simulation Setup

Fire Dynamics Simulator (FDS) (McGrattan et al., 2013) solves the thermally-driven fluid flow (low Ma number < 0.3). By use of the computational platform, our previous numerical works (Yang et al., 2022; Yang et al., 2019) successfully reproduced various flame modes of dual and triple flickering buoyant diffusion flames. Figure 1(a) shows the computational domain with a $16D$ side and $24D$ height square column. The central fuel jet (yellow area) has a diameter of $D = 0.01m$. Considering the computational cost and accuracy, we utilized a $160 \times 160 \times 240$ mesh and set uniform structure for the whole domain. The current domain and mesh are sufficient to capture the buoyance-induced flickering behavior, of which independence study was validated in detail in our previous study. The bottom ground (grey area) is a solid-wall boundary, set as impermeable, non-slip, and adiabatic. The central fuel jet is an inlet boundary.

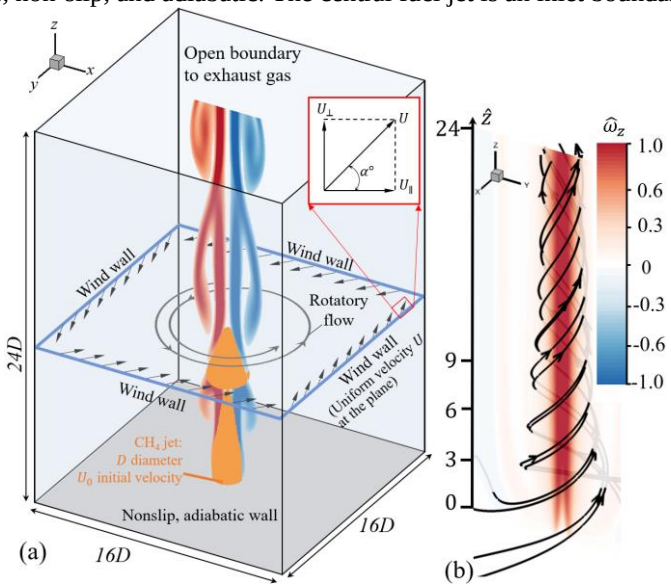

Figure 1 (a) The whole domain and its boundaries in the computational study; The externally swirling flow is injected a velocity $\boldsymbol{U} = (\boldsymbol{U}_{\perp}, \boldsymbol{U}_{\parallel})$, at an angle $\boldsymbol{\alpha}$ with the wind walls. (b) The vertical vorticity $\hat{\boldsymbol{\omega}}_{\boldsymbol{z}}$ in the $\boldsymbol{Z-X}$ plane for a nonreactive methane jet flow with externally rotating flow.

In the present study, a flickering buoyant diffusion flame is produced by jetting a methane flow with a uniform velocity profile of $U_0 = 0.165m/s$. The other remaining sides of the domain are set as the non-solid exterior, through which gases are allowed to flow freely. In pool flames and jet flames, the flow is predominated by buoyance due to a low initial momentum. Consequently, the chemistry is infinitely fast and the mixing-limited chemical reaction model is appropriate for simulating diffusion flames. Because the present flame scale is smal, we can negelect the effects of soot and radiation. Considering the local extinction, we used the Arrhenius equation (one-step finitely-rate) for the reaction rate:

$$\frac{d[CH_4]}{dt} = -Ae^{\frac{-E_a}{RT}}[CH_4]^a[O_2]^b \quad (1)$$

where $[CH_4]$ and $[O_2]$ are the methane and oxygen concentration in mol/cm^3, respectively; the parameters are prefactor of $A = 1.3$, avtivation energy of $Ea = 2.0 \times 10^5$ (J/mol), universal gas constant of $R = 8.3144$ (J/K·mol), and indexes of a=-0.3 and b=1.3, respectively.

Numerical Validation

In this section, we validated the present computational methodology and models and carried out a number of simulation runs of flickering buoyant diffusion flames with different U_0, D, and g in the quiescent environment (i.e., $R = 0$). In Fig. 2(a), the present results on flickering frequencies are well in line with previous experiments (Cetegen & Ahmed, 1993; Durox, Yuan, Baillot, & Most, 1995; Fang, Wang, Guan, Zhang, & Wang, 2016; Hamins, Yang, & Kashiwagi, 1992) and particularly predict the famous scaling relation of $St \sim \sqrt{Fr}$ (Byram & Nelson, 1970; Xia & Zhang, 2018), where $St = f_0 D/U_0$ and $Fr = U_0^2/gD$ are the Strouhal number and Froude number, respectively. The flickering flame produced computationally here is ejected from a hole in the bottom wall, but slightly different from those flames ejected from a tube

in previous studies. Consequently, the discrepancy results from the influence of the buoyance-induced flow at the flame base. In the weakly rotating conditions, the bottom wall can form a thin boundary flow to hardly influence on the flames flickering, because the toroidal vortex grows and sheds off downstream far from the bottom. However, the boundary effect becomes vital for flames in strong rotating flows.

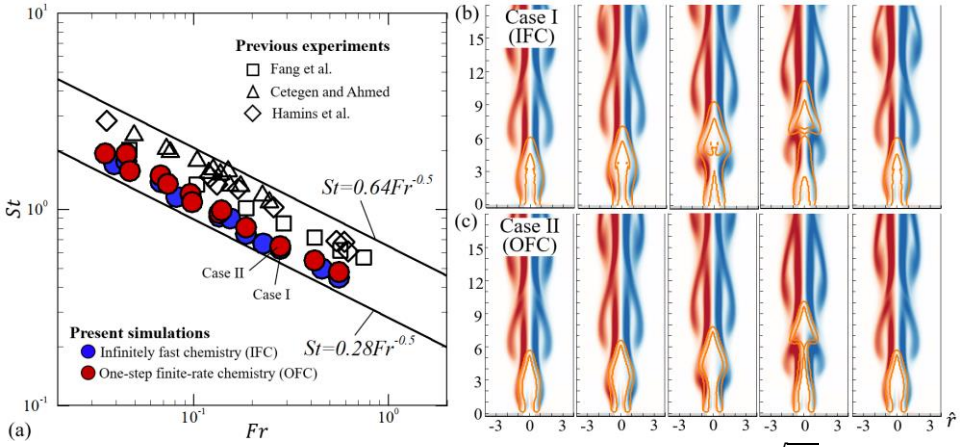

Figure 2 (a) The validation of single flickering flames with the scaling law of $St \sim \sqrt{Fr}$ and previous experiments. (b-c) The vorticity contour of a flickering buoyant diffusion flame with the mixing-limited chemical reaction model and the Arrhenius equation (eq.1).

Two cases are illustrated for same dynamical behaviors in Fig. 2(b)-2(c), respectively. The flickering buoyant diffusion flames with $D = 10$ mm and $g = 9.8$ m/s^2 have infinitely fast and one-step finitely-rate reactions. The toroidal vortex is formed due to the roll-up of the outside shear layer around the flame. The flame is pinched into two parts by the vortex. Besides, present results of $(0.5g - 1.5g)$ show that the gravity effect is significant in the flickering frequency. Therefore, we believe that the flicker of the present diffusion flames is controlled by buoyancy.

Numerical Implementation of a Rotating Flow

In Figure 1(a), the lateral sides are four "wind wall", on which the airflow is enjected to form rotating flows in the computational domain. The inlet velocity is set as $U = (U_\perp, U_\parallel)$, where $U_\perp$ and $U_\parallel$ are radial and tangential velocity components, respectively. Particularly, the inlet angle $\alpha = 45$ between the two components is fixed to avoid complex parametric studies. As shown in Fig. 1(b), the four inlet flows form a circulation in the central region and control the circulation intensity by changing velocity components. The approach is controllable and adjustable to generate a stable swirling flow.

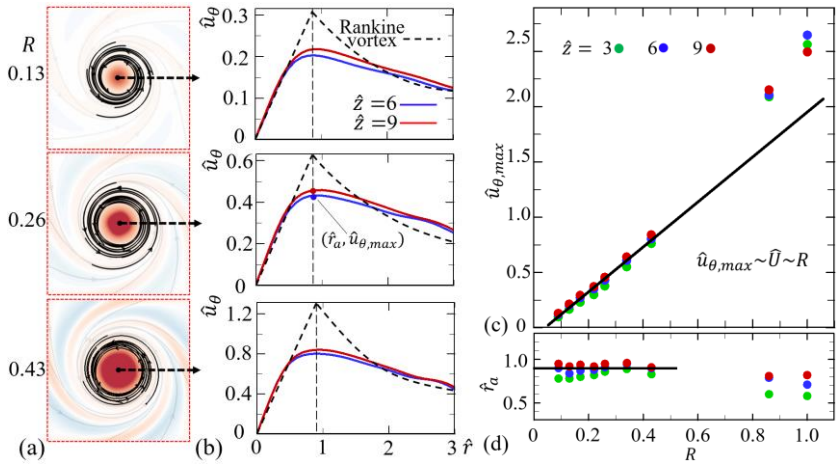

Figure 3 (a) The vertical vorticity $\hat{\omega}_z$ of a nonreactive methane jet flow in different swirling flows: horizontal sections ($X - Y$ planes). (b) The three cases correspond to different rotational conditions, in which the inlet wind is set up as $U_\perp = U_\parallel$ and $R = U/U_0 =$ 0.13, 0.26, and 0.43 at $Z/D = 6.0$ and 9.0. (c) The maximum azimuthal velocity $\hat{u}_{\theta,max}$ of vortex cores v.s. R. (d) The radial location $\hat{r}_a$ v.s. R.

We validated the present approach for swirling flow and compared different non-reacting flows from $R = 0$ to 1.0. With the imposed swirl intensifying, as shown in Fig. 3 (a)-3(b), the range of the central vortex core (denoted by the streamline-encompassed area) widens, and the intensity (denoted by the vertical vorticity) increases. In addition, the range and intensity of a swirling flow are almost kept the same from $3D$ to $9D$ in the vertical direction. Under different inlet winds, we can generate a variety of vortical strength upon the central flame.

In the present study, the calculated vortical flow can be assumed as the Rankine vortex (Kundu, Cohen, & Dowling, 2015), as its azimuthal velocity has a vortex core of radius $\hat{r}_a$, within which the relation of $\hat{u}_\theta(\hat{r}) \sim \hat{r}$ is and beyond which $\hat{u}_\theta(\hat{r}) \sim 1/\hat{r}$ exists. Fig. 3(c) shows that the maximum azimuthal velocity, $\hat{u}_\theta(\hat{r}_a) = \hat{u}_{\theta,max}$ has a linear relationship with $3.5\widehat{U}$, which increases by about $1.9R$. Besides, we have the flickering flame enbeded in the vortex core of the generated swirling flow due to the computational results of $\hat{r}_a \simeq 0.9$. Particularly, we found that R can be evaluated as $2\pi\hat{r}_a\hat{u}_{\theta,max}$, a dimensionaless parameter of circulation.

RESULTS AND DISCUSSION

Faster flicker of buoyant diffusion flames is observed in the previous experiments (Lei, Liu, & Satoh, 2015). In this section, the following questions will be focused: how a flickering flame behaves in an externally rotating flow; how its flickering frequency varies with R; what the physical mechanism of the faster flicker is. More details refer to our recent work (Yang & Zhang, 2023).

Flickering Flames in Weakly Rotating Flows

Figure 4(a) shows a $Re = 100$ diffusion flame in quiescent air, where the toroidal vortex around the flame is denoted by the spiral of streamlines. From a vortex-dynamics perspective, the flame-induced buoyancy provokes the growth of a shearing layer between the flame and the surroundings, and eventually results in a symmetric vortex (Xia & Zhang, 2018; Zhang, Xia, & Gao, 2021). The dimensional feature can be identified by the zero-value helicity density (Yang et al., 2019). Expescially, the axisymmetry of the present flames can retain during periodic flickering.

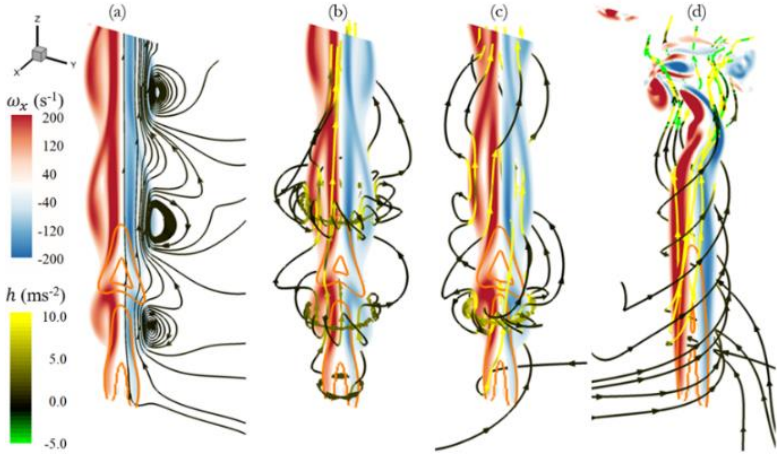

Figure 4 Four flickering flame cases of (a) $R = 0.0$ (quiescent air flow), (b-d) 0.09, 0.17, and 0.26 (rotating air flow), respectively. The heat release rate is used to identify the flame configuration. The vorticity ω_x is perpendicular to the $Y - Z$ plane. The streamlines are illustrated with the colorcode of helicity density $h = \vec{u} \cdot \vec{\omega}$.

Figure 4(b)-4(d) show the flickering buoyant diffusion flame in rotating flows with different strengths. By comparing these results, several important observations can be obtained for the swirling effect on a flickering buoyant diffusion flame. First, the morphology of flickering flames has changed, specifically, the main flame becomes slimmer and taller with the swirling strength increasing, while their shapes remain axisymmetric. Second, the shear layers around flames determine the flickering behavior. Their differences (the vorticity magnitude and the roll-up region) suggest that the rotating flow can change the flame pinch-off up to a certain strength. Third, the helicity density $h = \vec{u} \cdot \vec{\omega}$ is colored on the streamlines to facilitate the quantitative comparison, which denotes the nonorthogonality of the vorticity $\vec{\omega}$ and velocity $\vec{u}$ vectors. The results show that h in the shear layers increases from nearly 0 in Fig. 4(a), to about $0\sim5$ in Fig. 4(b), and about $0\sim10$ in Figure 4(c). In Fig. 4(d), the value h almost remains high ($\gtrsim 10$) in the flame and jumps abruptly between the negative and the positive in downstream regions. The stronger the surrounding swirl is, the higher h in the flame becomes. Four, the twisting of streamlines demonstrates the swirling effect on the vortex. The roll-up and the twist occur concurrently for forming the circumferentially spiral streamlines. When the external swirl is dominated, the vortex ring is suppressed or postponed to downstream locations and the vortex helix grows and twines around the flame, as shown in Fig. 4(d).

Figur. 5(a), 5(b), and 5(c) show the time-varying waves of Q(global quantity: overall heat production per time), u_z(local quantity: velocity component in z direction), and T(local quantity: temperature), respectively. They are used to determine the flickering frequency. Our results shows that the three variables have same period in all cases, but phase differences between different variables. The flickering frequency can be obtained via a fast Fourier transform of Q for 10s with a 1000 Hz sample. In Fig. 5(a), the value of Q oscillates at the frequency of $f_0 = 9.6$ Hz in $R = 0$ case, smaller than 10.6 Hz in R=0.17 case. The frequency increase suggests the early pinch-off of flame due to the externally rotating flow. Fig. 5(d) shows that higher R the rotating flow has, higher flickering frequency f the flame has. Clearly, the trend between f and R is monotonical and nonlinear.

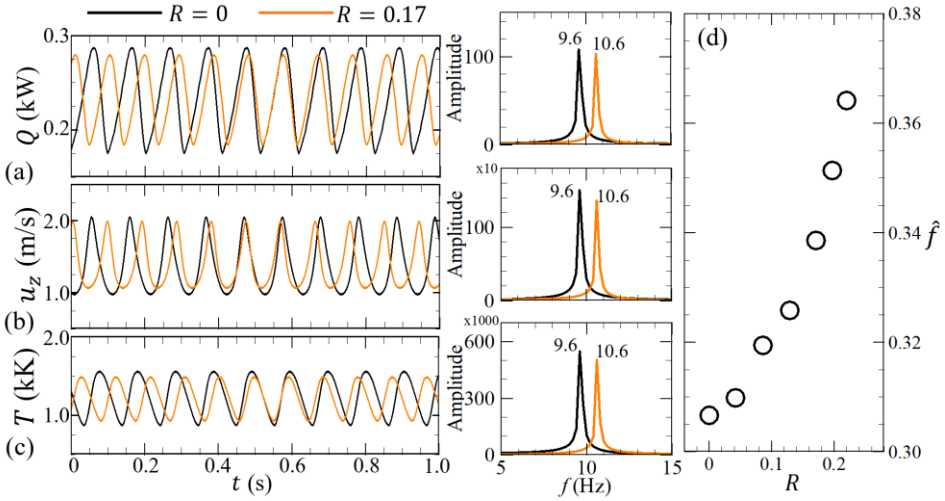

Figure 5 Time and frequency domain graphs of (a)Q, (b)u_z, and (c)T in the compared cases of $R = 0$ (black lines) and $R = 0.17$(orange lines). The local quantities are sampled at the point of $\hat{z} = 3$ and $\hat{r} = 0$. (d) The plot of the dimensionless frequency $\hat{f} = f/\sqrt{gD}$ and the swirling intensity R.

Vortex-dynamical Interpretation

To understand the faster flicker by rotating flows, we extended the previous theory (Xia & Zhang, 2018) and theoretically modeled the flickering frequency based on the physics that the shed-off of the toroidal vortex contributes the periodic behavior. To facilitate the comparison with the previous formular, we adopted the similar notation in the following discussion. Our primary concept is that the flame flickering phenomenon arises when the toroidal vortex grows up strongly and the corresponding circulation surpasses a constant value, which is considered to be an almost universally threshold and is presumed to remain relatively unchanged in the current weakly rotating environments. By theoretically deriving through three steps, we can obtain the frequency relation as follow:

$$\hat{f} = \frac{f}{\sqrt{g/D}} = \frac{1}{2C}\left(C_{jr}Fr + \sqrt{C_{jr}^2 Fr^2 + CC_hC_\rho}\right) \tag{2}$$

where C, C_{jr}, C_h, and C_ρ are prefactors relating to the threshold of vortex shedding, the initial fuel jet and rotational flow, the vertical motion of the toroidal vortex, and the ratio of flame and ambient density, respectively. Detail derivations refer to our recent work (Yang & Zhang, 2023).

Next, we consider the additional rotation of the ambient flow and obtain the frequency increase of flickering flames:

$$\Delta\hat{f} = \frac{f(R) - f(R=0)}{\sqrt{g/D}} = \frac{5\Phi}{C}R^2 \tag{3}$$

where Φ is about $1\sim2$, and the prefactor $C_r = 10R^2/\tilde{U}_0^2$ (relating to rotational flow) is used due to the prefactor $C_\theta = 2.11R$ (relating to azimuthal velocity within the vortex core) and $\hat{r}_c\overline{R} = 1.14$. Correspondingly, we can have a scaling law of $\Delta\hat{f}\sim R^2$. As shown in Fig. 6, the theoritical prediction is in a well line with the present computational results. Our recent work (Yang & Zhang, 2023) found that the correlation of $\Delta\hat{f}\sim R^2$ can be interpreated physically by the occurcance of the baroclinic effect $\nabla p \times \nabla\rho$, which strengthens the growth of toroidal vortices.

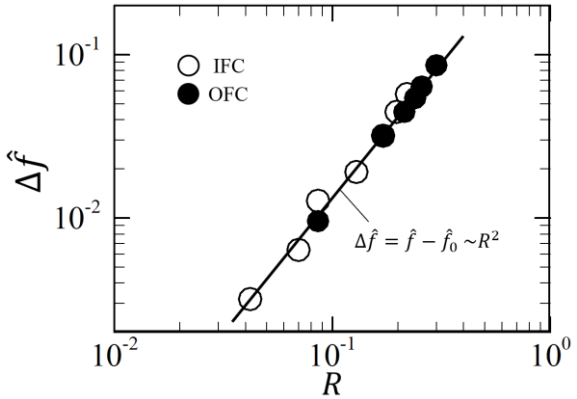

Figure 6 Validation of numerical results for the correlation of $\Delta\hat{f}\sim R^2$ proposed in theory.

Flames Modes in Strong Rotating Flow

In the section, a sufficiently large R causes various flame modes, where the flame phenomena are governed by different physical mechanisms with rotating flows becoming strong. As shown in Fig. 7, the flickering, oscillating, steady, and lifted flames forms under different vortex interactions. When R exceeds 0.26, the vortex shedding occurs downstream so that the flame has no pinch-off and just oscillates. At bigger $R = 0.43$, there is no roll-up in the upstream shear layer and the flame turns into a steady state. A very strong rotating flow ($R = 1.11$) causes local flame extinction and the flame detached to the bottom. By comparing heights between the vortex shedding-off and the flame for different cases, we found that increasing R strengthens the vortex and causes the shedding much downstream. Accordingly, the flame isn't pinched off and even is restricted to be steady. Particularly, enough strong swirling flow at a high R can form the inflow boundary layer at the bottom (Lei, Liu, Zhang, & Satoh, 2015), where the high shear rate leads to the local extinguishing and the lift-off of flame. More physical insights into those flame modes are given in our recent works (Yang, Ma, & Zhang, 2023; Yang & Zhang, 2023).

Figure 8 shows the phase portraits of those flame modes. It is seen that the trajectory of flickering flames is a closed ring. The oscillating has a closed trajectory upstream but the downstream is disorderly. The corresponding vorticity contour also presents that the shear layer around the flame develops into fragments far from the flame. For the steady flame, the phase portrait of the upstream becomes a point, while that of the downstream shows a slight distribution. However, the lifted flame has a nearly motionless phase trajectory, which means that the whole flow field turns steady. It should be noted that our simulations capture the two special flames, where one behaves in a spiral way and the other lifts off with a vortex bubble. For more details results refer to our preprint (Yang et al., 2023). The two cases can occur under the different Froude number Fr, rotating intension R, and inlet angle α, which deserve further studies.

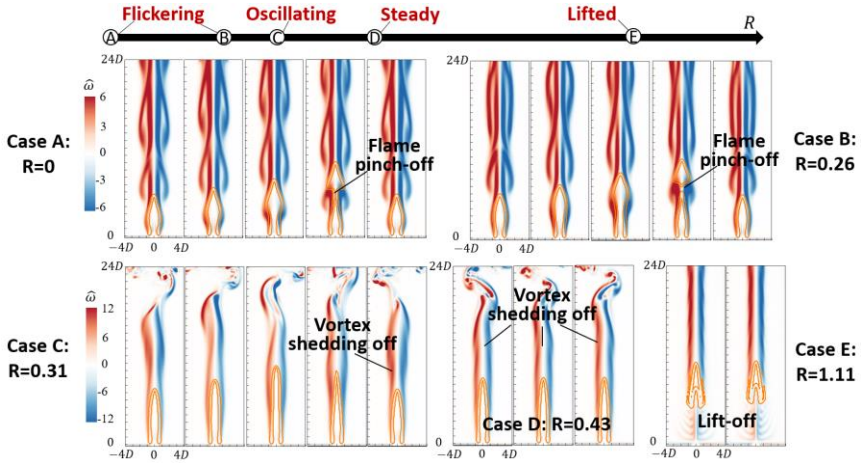

Figure 7 Snapshots of the flickering buoyant diffusion flame in different rotating flows: five cases at $R = 0,\ 0.26,\ 0.31,\ 0.43,\ 1.11$.

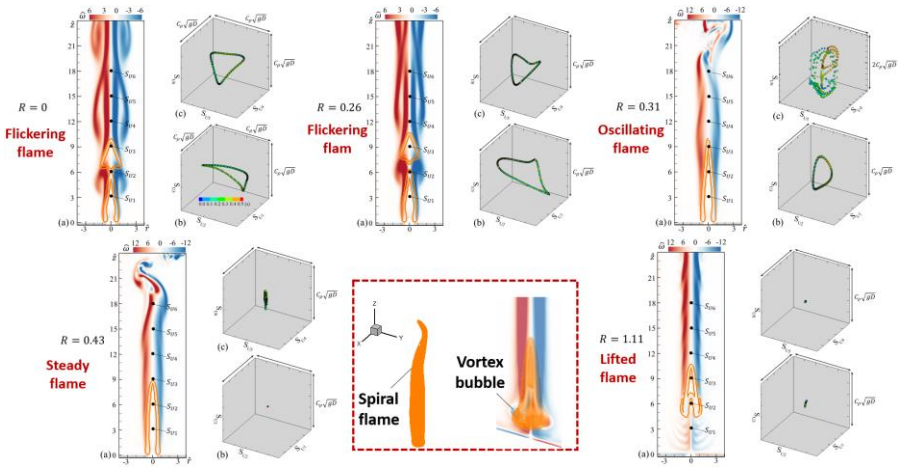

Figure 8 Phase portraits of different flame modes (a), including flickering, oscillating, steady, and lifted flames. Two cases for spiral and vortex-bubble flames. The phase spaces (b) and (c) of each mode correspond to the upstream and downstream zones, where the axial velocities at three fixed points along the axis (i.e. $S_{U1} - S_{U2} - S_{U3}$ and $S_{U4} - S_{U5} - S_{U6}$) are plotted as the coordinates of phase space.

CONCLUSIONS

In this study, we computationally and theoretically investigated the small-scale flickering buoyant diffusion flames under externally rotating flow conditions. The present work shows that the ambient flow with a swirl can strengthen the periodically up and down motion of diffusion flame, which agrees with the previous experimental observations (Lei, Liu, & Satoh, 2015). The scaling theory for interpreting the frequency increase can be simplified into that of previous theory without swiring flow. The present computational results agree very well with the correlation of $\Delta\hat{f} = \hat{f} - \hat{f}_0 \sim R^2$. Physically, the growth of toroidal vortices is strengthened by an additional source due to the baroclinic effect $\nabla p \times \nabla \rho$. At large R, six distinct flames modes are illustrated by their phase portraits and their underlying mechanisms deserve further study.

ACKNOWLEDGMENTS

This work is financially supported by the National Natural Science Foundation of China (No. 52176134) and partially by the APRC-CityU New Research Initiatives/Infrastructure Support from Central of City University of Hong Kong (No. 9610601).

REFERENCES

Buckmaster, J., & Peters, N. (1988). The infinite candle and its stability—a paradigm for flickering diffusion flames. *Proceedings of the Combustion Institute, 21*(1), 1829-1836.

Byram, G. M., & Nelson, R. M. (1970). The modeling of pulsating fires. *Fire Technology, 6*(2), 102-110.

Cetegen, B. M., & Ahmed, T. A. (1993). Experiments on the periodic instability of buoyant plumes and pool fires. *Combustion and Flame, 93*(1-2), 157-184.

Cha, J., & Sohrab, S. (1996). Stabilization of premixed flames on rotating Bunsen burners. *Combustion and Flame, 106*(4), 467-477.

Chamberlin, D. S., & Rose, A. (1948). The flicker of luminous flames. *Proceedings of the Combustion Institute, 1-2*, 27-32.

Coenen, W., Kolb, E. J., Sánchez, A. L., & Williams, F. A. (2019). Observed dependence of characteristics of liquid-pool fires on swirl magnitude. *Combustion and Flame, 205*, 1-6.

Durox, D., Yuan, T., Baillot, F., & Most, J. (1995). Premixed and diffusion flames in a centrifuge. *Combustion and Flame, 102*(4), 501-511.

Fang, J., Wang, J.-w., Guan, J.-f., Zhang, Y.-m., & Wang, J.-j. (2016). Momentum-and buoyancy-driven laminar methane diffusion flame shapes and radiation characteristics at sub-atmospheric pressures. *Fuel, 163*, 295-303.

Gotoda, H., Asano, Y., Chuah, K. H., & Kushida, G. (2009). Nonlinear analysis on dynamic behavior of buoyancy-induced flame oscillation under swirling flow. *International Journal of Heat and Mass Transfer, 52*(23-24), 5423-5432.

Gotoda, H., Ueda, T., Shepherd, I. G., & Cheng, R. K. (2007). Flame flickering frequency on a rotating Bunsen burner. *Chemical Engineering Science, 62*(6), 1753-1759.

Hamins, A., Yang, J., & Kashiwagi, T. (1992). An experimental investigation of the pulsation frequency of flames. *Proceedings of the Combustion Institute, 24*(1), 1695-1702.

Kundu, P. K., Cohen, I. M., & Dowling, D. R. (2015). *Fluid mechanics*. Cambridge: Academic press.

Lei, J., Liu, N., & Satoh, K. (2015). Buoyant pool fires under imposed circulations before the formation of fire whirls. *Proceedings of the Combustion Institute, 35*(3), 2503-2510.

Lei, J., Liu, N., Zhang, L., & Satoh, K. (2015). Temperature, velocity and air entrainment of fire whirl plume: A comprehensive experimental investigation. *Combustion and Flame, 162*(3), 745-758.

McGrattan, K., Hostikka, S., McDermott, R., Floyd, J., Weinschenk, C., & Overholt, K. (2013). Fire dynamics simulator user's guide. *NIST special publication, 1019*(6), 1-339.

Moreno-Boza, D., Coenen, W., Sevilla, A., Carpio, J., Sánchez, A., & Liñán, A. (2016). Diffusion-flame flickering as a hydrodynamic global mode. *Journal of Fluid Mechanics, 798*, 997-1014.

Sheu, W., Sohrab, S., & Sivashinsky, G. (1990). Effect of rotation on Bunsen flame. *Combustion and Flame, 79*(2), 190-198.

Xia, X., & Zhang, P. (2018). A vortex-dynamical scaling theory for flickering buoyant diffusion flames. *Journal of Fluid Mechanics, 855*, 1156-1169.

Yang, T., Chi, Y., & Zhang, P. (2022). Vortex interaction in triple flickering buoyant diffusion flames. *Proceedings of the Combustion Institute*, (in press).

Yang, T., Ma, Y., & Zhang, P. (2023). Dynamical Behaviors of Small-scale Buoyant Diffusion Flame Oscillators in Externally Swirling Flows. *arXiv preprint arXiv:2303.15789*.

Yang, T., Xia, X., & Zhang, P. (2019). Vortex-dynamical interpretation of anti-phase and in-phase flickering of dual buoyant diffusion flames. *Physical Review Fluids, 4*(5), 053202.

Yang, T., & Zhang, P. (2023). Faster flicker of buoyant diffusion flames by weakly rotatory flows. *Theoretical and Computational Fluid Dynamics*, 1-18.

Zhang, H., Xia, X., & Gao, Y. (2021). Instability transition of a jet diffusion flame in quiescent environment. *Proceedings of the Combustion Institute, 38*(3), 4971-4978.